Continuously tunable sub-half-wavelength localization via coherent control of spontaneous emission*

Wang Fei(王 飞)[a)†], Gong Cheng(龚 成)[b)], Tan Xin-Yu(谭新玉)[a)], and Shi Wen-Xing(石文星)[c)]

[a)] College of Science, New Energy Research Institute, China Three Gorges University, Yichang 443002, China

[b)] State Key Laboratory of High Field Laser Physics, Shanghai Institute of Optics and Fine Mechanics, Chinese Academy of Sciences, Shanghai 201800, China

[c)] School of Physics & Information Engineering, Jianghan University, Wuhan 430056, China

(Received 22 March 2012; revised manuscript received 22 May 2012)

We propose a continuously tunable method of sub-half-wavelength localization via the coherent control of the spontaneous emission of a four-level Y-type atomic system, which is coupled to three strong coupling fields including a standing-wave field together with a weak probe field. It is shown that the sub-half-wavelength atomic localization is realized for both resonance and off-resonance cases. Furthermore, by varying the probe detuning in succession, the positions of the two localization peaks are tuned continuously within a wide range of probe field frequencies, which provides convenience for the realization of sub-half-wavelength atomic localization experimentally.

Keywords: sub-half-wavelength localization, spontaneous emission, atomic coherence

PACS: 42.50.Gy, 32.80.Qk **DOI:** 10.1088/1674-1056/21/11/114206

1. Introduction

The atomic localization has attracted a great deal of interest due to its widely application in laser cooling and trapping,[1−5] Bose–Einstein condensation,[6−8] atom lithography,[9,10] and so on. Several optical methods for atomic localization have been proposed. For example, Storey *et al.* proposed a scheme to realize the localization based on the measurement of the phase shift of the standing wave.[11,12] Later on, it is demonstrated that the resonance imaging methods can be used to localize the atoms.[13,14] A number of schemes for the atomic localization have been presented based on the electromagnetically induced transparency,[15] the interference of double-state resonance,[16] the coherent manipulation of the Raman gain process,[17] the polychromatic excitation,[18−20] and the coherence control of spontaneous emission,[21−26] recently. Besides, Ivanov *et al.* have proposed a scheme for the two-dimensional atom localization in a four-level tripod system,[27] they demonstrated a high-precision localization due to the measurement of population in the upper state or in any ground state.

In particular, the coherence control of spontaneous emission has been regarded as a useful way to investigate the atomic localization. Zubairy *et al.*[21] proposed a scheme to localize a three-level atom based on the Autler–Townes spontaneous spectrum, wherein a classical strong standing-wave field was employed to couple the auxiliary level. Due to the Autler–Townes splitting dependence on position, detection of the spontaneously emitted photon provides position information of the atom along with the standing-wave field. They also showed that the detuning effects between the atomic transition and the classical standing-wave field were important for the atomic localization in a three-level atom,[22] whose position information was obtained by measuring the Autler–Townes spontaneous spectrum in the upper-level coupling case. For the two schemes, there were four equally probable localization peaks existing in a unit wavelength domain of the standing wave, indicating that the detection probability was confined to 25%.

In order to enhance the precision in atomic localization, the phase control of the Autler–Townes spontaneous spectrum was adopted by Zubairy *et al.*[23−25] in a four-level atomic system, where the excited state of the probe transition was coupled to two auxiliary

*Project supported by the National Natural Science Foundation of China (Grant Nos. 11104163 and 11047011) and the Science Foundation of Hubei Province, China (Grant No. 2010CDZ055).

†Corresponding author. E-mail: feiwang202@163.com

© 2012 Chinese Physical Society and IOP Publishing Ltd

levels in a loop configuration using one standing-wave field and two traveling-wave fields. By controlling the amplitudes and the phases of the driven fields, two localization peaks appeared in the half wavelength region through the measurement of the spontaneous emitted photon or the weak field absorption. As a result, the detecting probability reached 50%. This is termed as the sub-half-wavelength localization. In the schemes mentioned above, the probe field detuning plays an important role in the atomic localization. In the absence of probe detuning, the conditional probability distribution is space invariant, so those schemes are no longer available for the atomic localization. In contrast, a scheme has been proposed based on the resonant interaction via detecting the absorption spectrum.[26] When the probe field is resonant with the atomic transition, the atom is localized at the nodes of the standing-wave field in the sub-half-wavelength domain with 50% detecting probability. However, as the probe field detuning increases, the detecting probability is reduced and vanishes eventually.

As referred above, the atomic localization was realized on the condition of either resonance or off-resonance. A question naturally arises, will the sub-half-wavelength atomic localization happen under both conditions over a wide range of probe field frequencies in a scheme? In this paper, we show that the sub-half-wavelength atomic localization is achievable under both conditions. The significant interesting features we find in the present scheme are as follows. Firstly, the positions of the two localization peaks are continuously tunable by changing the probe detuning in succession. The position curve versus the probe detuning is similar to the sine curve. Secondly, if the probe detuning is changed from negative to positive, the two localization peaks appear or vanish symmetrically at the nodes of the standing-wave field. Thirdly, as the absolute value of the probe detuning decreases, the width of the peak becomes narrower. In addition, the sub-half-wavelength localization depends on the collective phase of the three strong applied fields, which has been realized in the previous work.[24,25] In short, in the present scheme, the conditions for the localization are relaxed, which is useful for experimental control.

2. Model and equations

As schematically illustrated in Fig. 1, a four-level Y-configuration atom model is considered, which has two excited states: an intermediate state, and a ground state. The atom moving in the z direction passes through a classical standing-wave light field in a cavity aligned along the x direction. The standing-wave laser field is applied to the dipole-allowed transition $|3\rangle$–$|1\rangle$. A traveling-wave laser field and a microwave field are applied to the dipole-allowed transition $|2\rangle$–$|1\rangle$ and the dipole-forbidden transition transition $|3\rangle$–$|2\rangle$, respectively. The upper transitions form a closed loop. A weak probe field is applied to the lower probe transition $|1\rangle$–$|0\rangle$. The four fields are written as $E_j\,\mathrm{e}^{-\mathrm{i}(v_j t+\phi_j)}+\mathrm{c.c.}$ $(j=0,1,2,\mathrm{d})$, where E_j, v_j, and ϕ_j are the amplitudes, the frequencies, and the initial phases, respectively. The position-dependent standing-wave component $E_1=E_1^{\mathrm{s}}\sin(kx)$ has wave vector $k=2\pi/\lambda$, where λ is the wave length of the standing-wave field. Assuming the center-of-mass position of the atom to be a constant along the direction of the standing wave, and neglecting the kinetic term of the atom in the Raman–Nath approximation,[28] we derive the master equation for the atom–field interaction system in an appropriate rotating frame and under the dipole approximation

$$\dot{\rho} = -\frac{\mathrm{i}}{\hbar}[H,\rho]+\mathscr{L}_{13}\rho+\mathscr{L}_{12}\rho+\mathscr{L}_{01}\rho, \tag{1}$$

$$H = \hbar\Delta_{\mathrm{p}}\sigma_{00}-\hbar\Big[\Omega_1\sin(kx)\,\sigma_{31}+\Omega_2\sigma_{21} + \Omega_{\mathrm{d}}\,\mathrm{e}^{-\mathrm{i}\phi}\sigma_{32}+\Omega_{\mathrm{p}}\sigma_{10}+\mathrm{H.c.}\Big], \tag{2}$$

where Δ_{p} is the probe detuning between the atomic transition frequency ω_{10} and the weak field frequency ω_{p}, (here we assume that the three strong applied fields are resonant with the corresponding transitions) $\Omega_1\sin(kx)$ is the position-dependent half Rabi frequency of the standing-wave field, Ω_2, Ω_{d}, and Ω_{p} are half Rabi frequencies associated with the traveling-wave field, the micro-wave field, and the probe field, respectively, and $\phi=\phi_1+\phi_2-\phi_{\mathrm{d}}$ is the collective phase of the three applied fields. The phase of the probe field is not considered, because it has no effect. The damping terms take the form

$$\mathscr{L}_{ij}\rho=\gamma_{kj}\left(2\sigma_{jk}\rho\sigma_{kj}-\sigma_{kk}\rho-\rho\sigma_{kk}\right), \tag{3}$$

where $2\gamma_{kj}$ represents the atom decay rate from state $|k\rangle$ to state $|j\rangle$, $\sigma_{kl}=|k\rangle\langle l|$ is the atomic projection operator for $k=l$ and the flip operator for $k\neq l$

$(k,l=0,1,2,3)$. In the following, we set $\gamma_{31}=\gamma_1$, $\gamma_{21}=\gamma_2$, $\gamma_{10}=\gamma_0$. The set of equations for the density matrix elements are derived from Eqs. (1)–(3) as

$$\begin{aligned}
\dot{\rho}_{33} &= -2\gamma_1\rho_{33}+\mathrm{i}\Omega_1\left(\rho_{13}-\rho_{31}\right)\\
&\quad+\mathrm{i}\Omega_\mathrm{d}\left(\rho_{23}\,\mathrm{e}^{-\mathrm{i}\phi}-\rho_{32}\,\mathrm{e}^{\mathrm{i}\phi}\right),\\
\dot{\rho}_{22} &= -2\gamma_2\rho_{22}+\mathrm{i}\Omega_2\left(\rho_{12}-\rho_{21}\right)\\
&\quad+\mathrm{i}\Omega_\mathrm{d}\left(\rho_{32}\,\mathrm{e}^{\mathrm{i}\phi}-\rho_{23}\,\mathrm{e}^{-\mathrm{i}\phi}\right),\\
\dot{\rho}_{00} &= 2\gamma_0\rho_{11}+\mathrm{i}\Omega_\mathrm{p}\left(\rho_{10}-\rho_{01}\right),\\
\dot{\rho}_{23} &= -\left(\gamma_1+\gamma_2\right)\rho_{23}-\mathrm{i}\Omega_1\rho_{21}+\mathrm{i}\Omega_2\rho_{13}\\
&\quad+\mathrm{i}\Omega_\mathrm{d}\,\mathrm{e}^{\mathrm{i}\phi}\left(\rho_{33}-\rho_{22}\right),\\
\dot{\rho}_{13} &= -\left(\gamma_0+\gamma_1\right)\rho_{13}+\mathrm{i}\Omega_1\left(\rho_{33}-\rho_{11}\right)\\
&\quad+\mathrm{i}\Omega_2\rho_{23}+\mathrm{i}\Omega_\mathrm{p}\rho_{03}-\mathrm{i}\Omega_\mathrm{d}\rho_{12}\,\mathrm{e}^{\mathrm{i}\phi},\\
\dot{\rho}_{03} &= -\left(\gamma_1-\mathrm{i}\Delta_\mathrm{p}\right)\rho_{03}-\mathrm{i}\Omega_1\rho_{01}+\mathrm{i}\Omega_\mathrm{p}\rho_{13}\\
&\quad-\mathrm{i}\Omega_\mathrm{d}\rho_{02}\,\mathrm{e}^{\mathrm{i}\phi},\\
\dot{\rho}_{12} &= -\left(\gamma_0+\gamma_2\right)\rho_{12}+\mathrm{i}\Omega_1\rho_{32}+\mathrm{i}\Omega_2\left(\rho_{22}-\rho_{11}\right)\\
&\quad+\mathrm{i}\Omega_\mathrm{p}\rho_{02}-\mathrm{i}\Omega_\mathrm{d}\rho_{13}\,\mathrm{e}^{-\mathrm{i}\phi},\\
\dot{\rho}_{02} &= -\left(\gamma_2-\mathrm{i}\Delta_\mathrm{p}\right)\rho_{02}-\mathrm{i}\Omega_2\rho_{01}+\mathrm{i}\Omega_\mathrm{p}\rho_{12}\\
&\quad-\mathrm{i}\Omega_\mathrm{d}\rho_{03}\,\mathrm{e}^{-\mathrm{i}\phi},\\
\dot{\rho}_{01} &= -\left(\gamma_0+\mathrm{i}\Delta_\mathrm{p}\right)\rho_{01}-\mathrm{i}\Omega_1\rho_{03}-\mathrm{i}\Omega_2\rho_{02}\\
&\quad+\mathrm{i}\Omega_\mathrm{p}\left(\rho_{11}-\rho_{00}\right),
\end{aligned}\tag{4}$$

together with the complex conjugates of the above equations. The set of equations of motion for the expectation values of the atomic operators are derived from Eq. (4) as

$$\frac{\mathrm{d}}{\mathrm{d}t}\boldsymbol{X}\left(t\right)=\boldsymbol{Q}\boldsymbol{X}\left(t\right)+\boldsymbol{R},\tag{5}$$

where $\boldsymbol{X}\left(t\right)=(\langle\sigma_{33}\rangle,\langle\sigma_{22}\rangle,\langle\sigma_{00}\rangle,\langle\sigma_{32}\rangle,\langle\sigma_{31}\rangle,\langle\sigma_{30}\rangle,\langle\sigma_{21}\rangle,\langle\sigma_{20}\rangle,\langle\sigma_{10}\rangle,\langle\sigma_{01}\rangle,\langle\sigma_{02}\rangle,\langle\sigma_{12}\rangle,\langle\sigma_{03}\rangle,\langle\sigma_{13}\rangle,\langle\sigma_{23}\rangle)^{\mathrm{T}}$ is a column vector, $\boldsymbol{Q}$ is a 15×15 matrix, and $\boldsymbol{R}$ is a column vector. The $\boldsymbol{Q}$ and $\boldsymbol{R}$ can be easily derived. The steady-state spontaneous emission spectrum from the $|1\rangle\rightarrow|0\rangle$ transition is given by

$$\begin{aligned}
S\left(\omega,x\right) &= \gamma_0 u\left(\boldsymbol{r}\right)\mathrm{Re}\int_0^\infty\mathrm{d}\tau\\
&\quad\times\lim_{t\rightarrow\infty}\left\langle\delta\sigma_{10}\left(t+\tau\right)\delta\sigma_{01}\left(t\right)\right\rangle\,\mathrm{e}^{-\mathrm{i}\omega\tau},
\end{aligned}\tag{6}$$

where $u\left(\boldsymbol{r}\right)=\left(3/8\pi\right)\sin^2\theta$ is a normalization constant, θ is the angle between the observation direction $\boldsymbol{r}$ and the atomic dipole moment of the $|0\rangle$–$|1\rangle$ transition, and $\delta\sigma_{10}\left(\tau\right)=\sigma_{10}\left(\tau\right)-\left\langle\sigma_{10}\left(\infty\right)\right\rangle$ represents the deviation of the dipole polarization operator $\sigma_{10}\left(\tau\right)$ from its mean steady value. In order to calculate the correlation spectrum, a column vector $\boldsymbol{Y}\left(\tau\right)$ is introduced, and its elements are two-time correlation functions $Y_k\left(\tau\right)=\left\langle\delta\sigma_{mn}\left(\tau\right)\delta\sigma_{01}\left(0\right)\right\rangle$. We should note that the order of elements $Y_k\left(\tau\right)$ is the same as that of $X_k\left(\tau\right)$. According to the quantum regression theory,[29] we can obtain the equation of $\boldsymbol{Y}\left(\tau\right)$ as

$$\frac{\mathrm{d}}{\mathrm{d}\tau}\boldsymbol{Y}\left(\tau\right)=\boldsymbol{Q}\boldsymbol{Y}\left(\tau\right),\tag{7}$$

which can be solved by making use of matrix $\boldsymbol{Q}$. Then we can get the spontaneous spectrum

$$S\left(\omega,x\right)=r_0u\left(\boldsymbol{r}\right)\mathrm{Re}\sum_{k=1}^{15}U_{9k}\left(\mathrm{i}\tilde{\omega}\right)Y_k\left(0\right),\tag{8}$$

where $\tilde{\omega}=\omega-\omega_{10}$ is the detuning between the scattered light frequency ω and the atomic resonance frequency ω_{10}, $Y_k\left(0\right)$ is the initial values of the elements of vector $\boldsymbol{Y}\left(\tau\right)$, and U_{9k} is the elements of the ninth row in the matrix $\boldsymbol{U}=\left(\mathrm{i}\tilde{\omega}\boldsymbol{I}-\boldsymbol{Q}\right)^{-1}$, with $\boldsymbol{I}$ being a unit matrix.

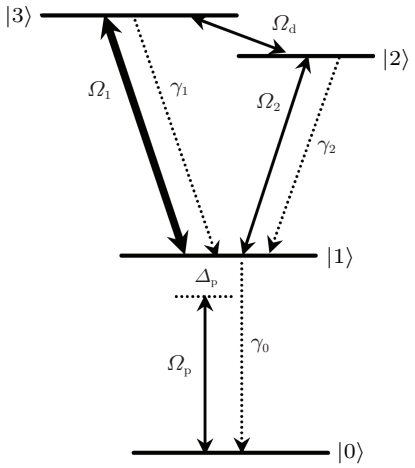


Fig. 1. Energy level structure of the Y-type atom.

The driven atom radiates spontaneously, and the detector detects the spontaneously emitted photons. The spectrum of the spontaneously emitted photons mimics the position probability of the center-of-mass motion of the atom. The conditional position distribution of the atom as a function of position x and frequency ω is given by[21,22]

$$W\left(\omega,x\right)=\left|\mathscr{N}\right|^2\left|f\left(x\right)\right|^2S\left(\omega,x\right),\tag{9}$$

where $\mathscr{N}$ is a normalized factor, $f\left(x\right)$ is the center-of-mass function of the atom and is assumed to be nearly a constant over many wavelengths of the standing-wave field.

3. Numerical results and discussion

When the spontaneously emitted photons are measured at a fixed frequency, the conditional position probability is only a function of position $W(x)$. Here, we present the numerical results of the probability distribution. The Rabi frequencies, the decay rates, the frequencies, and the detunings are scaled in units of decay rate γ_0. For simplicity, we assume all of the four half Rabi frequencies (Ω_1, Ω_2, Ω_d, Ω_p) to be real and that the probe field is much weaker than the applied fields. In our discussion, the parameters are set as $\gamma_1 = \gamma_2 = 0.2\gamma_0$, $\Omega_1 = \Omega_2 = \Omega_d = \Omega = 20\gamma_0$, and $\Omega_p = \gamma_0$.

The conditional position probability $W(x)$ is plotted as a function of kx ($-\pi \leq kx \leq \pi$) and probe detuning Δ_p for the collective phase $\phi = 0$, as shown in Fig. 2. It is shown that the atomic localization occurs over a wide range of probe detunings. As the probe detuning Δ_p changes from $-20\gamma_0$ to $20\gamma_0$, two localization peaks appear in each of the two half-wavelength regions, while they appear at the nodes of the standing-wave field when $\Delta_p = 0$. It means that the atomic localization is realized with a detecting probability of 50%. Several characteristics are found. (i) The positions of the sub-half-wavelength localization peaks are continuously tuned when the probe detuning changes in succession. In the region of $-20\gamma_0 < \Delta_p < 0$, the two localization peaks appear in the right side of the half-wavelength region. The distance between the two peaks increases continuously as the probe detuning changes. When $0 < \Delta_p < 20\gamma_0$, the two localization peaks switch from the right side to the left side, and the interval decreases successively. The position curve shown in Fig. 2 is similar to a sine curve. (ii) The two localization peaks appear symmetrically in two half-wavelength regions. When the probe detuning is tuned from negative to positive, the two peaks are symmetrical about the nodes of the standing-wave field. (iii) The widths of the localization peaks become narrower as the absolute value of the probe detuning decreases, implying that the higher precision is obtained during this process. Accordingly, in the present scheme, the position as well as the precision of the spatial resolution of the atomic localization can be controlled only by modifying the probe detuning.

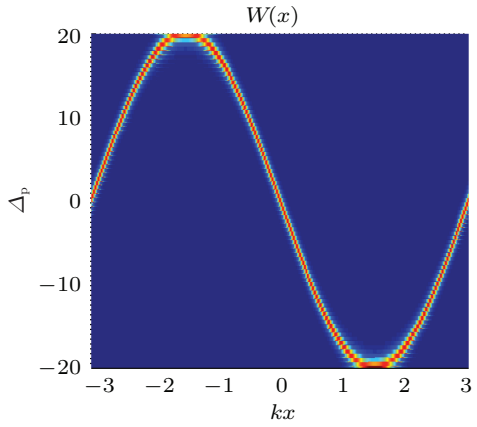


Fig. 2. (colour online) The positions of the two localization peaks as a function of kx ($-\pi \leq kx \leq \pi$) and probe detuning for the collective phase $\phi = 0$. The other parameters are chosen as $\gamma_1 = \gamma_2 = 0.2\gamma_0$, $\Omega_1 = \Omega_2 = \Omega_d = \Omega = 20\gamma_0$, and $\Omega_p = \gamma_0$.

For a further insight into the characteristics found above, we plot $W(x)$ as a function of kx ($-\pi \leq kx \leq \pi$) in Fig. 3 by taking the probe detuning $\Delta_p = -15\gamma_0$, $-5\gamma_0$, 0, $5\gamma_0$, $15\gamma_0$ respectively. Under the resonance condition, i.e., $\Delta_p = 0$, the atom is localized at the nodes of the standing-wave field. The two localization peaks for $\Delta_p = -15\gamma_0$ (blue dotted line) and $-5\gamma_0$ (red dotted line) are symmetrical with the peaks of $\Delta_p = 15\gamma_0$ (blue solid line) and $5\gamma_0$ (red solid line) about the position of $\Delta_p = 0$ (black solid line), respectively. The two peaks have full widths of 0.1 for $\Delta_p = \pm 15\gamma_0$ and 0.06 for $\Delta_p = \pm 5\gamma_0$. It is evident that the width of the localization peak for the latter case is narrower than that for the former one. This gives rise to a higher spatial resolution in the position distribution. Since the amplitudes of the three strong applied fields are equal to each other, in the dressed state picture, the energy separations of the three dressed states are identical. The coherence induced symmetrical triplet splitting results in the selective elimination of spontaneous emission. This is

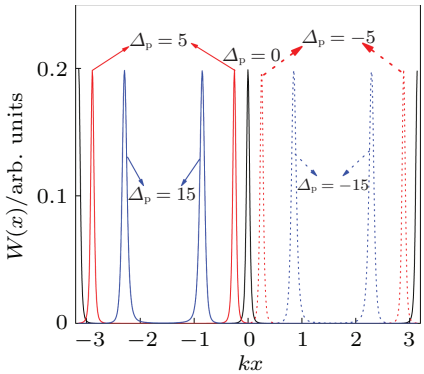


Fig. 3. (colour online) The 2D demonstration of Fig. 2 for chosen probe detuning Δ_p.

the essential reason for the sub-half-wavelength localization occurring periodically and symmetrically.

In addition, as shown in Fig. 4, the detecting probability can be controlled by varying the collective phase of the three applied fields. We show the conditional position probability distributions $W(x)$ for the phases $\phi = 0$, $\pi/2$, $3\pi/2$, π and different probe detuning values $\Delta_{\rm p} = 10$, 20. The other parameters are the same as those in Fig. 2. When $\Delta_{\rm p} = 10$, $\phi = 0$ (Fig. 4(a-1)), two localization peaks are confined in the left half-wavelength domain ($-\pi \leq kx \leq 0$), whereas no localization peaks appear in the right half-wavelength domain ($0 \leq kx \leq \pi$). This case is termed as the sub-half-wavelength localization. With the detuning increased to $\Delta_{\rm p} = 20$, $\phi = 0$ (Fig. 4(b-1)), the two adjacent peaks overlapping with each other finally evolve into one. For this case, the probability peak is wide. When the collective phase is varied from $\phi = 0$ to $\phi = \pi/2$ or $3\pi/2$ (Figs. 4(a-2) and 4(b-2)), the distribution probability peaks vanish, the spontaneous emission is negligibly weak. This is based on the fact that the phase control leads to the quenching in the spontaneous emission spectrum.[24,25] When the collective phase is set to be $\phi = \pi$, the conditional position probability distribution $W(x)$ switches symmetrically from one side to the other with a fixed detecting probability, as shown in Figs. 4(a-3) and 4(b-3)).

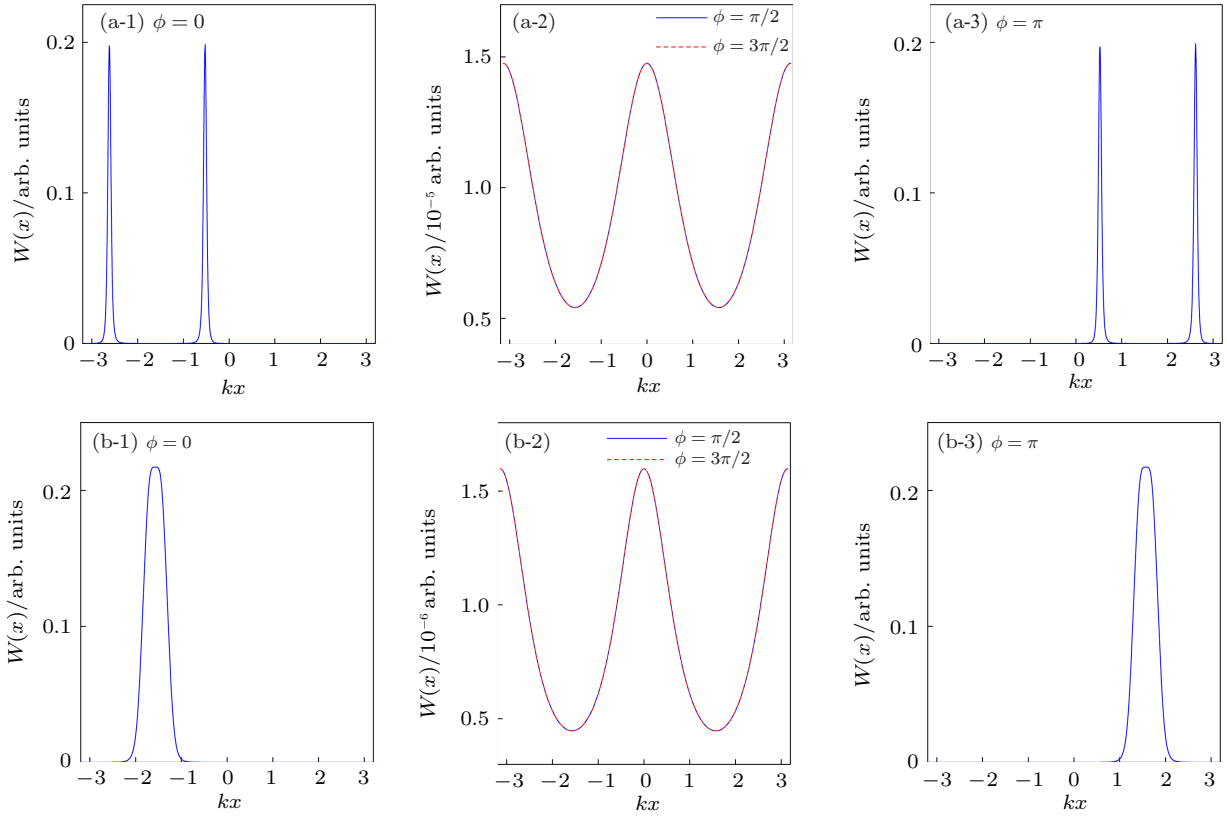


Fig. 4. (colour online) Conditional position probability distribution $W(x)$ as a function of kx ($-\pi \leq kx \leq \pi$) for different values of collective phase ϕ and detuning values (a) $\Delta_{\rm p} = 10$ (b) $\Delta_{\rm p} = 20$. The other parameters are the same as those in Fig. 2.

Finally, we make a comparison with the previous work. In our scheme, the advantage is beyond the realization of sub-half-wavelength. The positions of the two localization peaks are continuously controllable. In addition to the dominant feature, there are several differences between our work and the others. In Ref. [24], the localization of the atom via spontaneous emission is required to be prepared in a specific excited state, which is hard to realize in experiment. However, in our scheme, a weak probe field is used to excite the population into the excited state. The initial preparation of the atom in the specific excited state is not necessary. In Refs. [21]–[25], the sub-half-wavelength localization is realized when the probe field is not resonant with the atom over a narrow region. In Ref. [26], the atom is localized at the nodes of the standing-

wave field under the resonance condition, whereas the detecting precision decreases as the probe detuning increases. Nevertheless, in our scheme, the sub-half-wavelength localization is realized under both conditions, the conditions for sub-half-wavelength atomic localization are relaxed extensively. It can improve the experimental accessibility and controllability.

4. Conclusion

In summary, we propose an effective scheme for the sub-half-wavelength localization, wherein the positions and the precision of the localization peaks are continuously controllable by varying the probe detuning. The mechanism is closely related to the coherence induced symmetrical triplet splitting results in the selective elimination of the spontaneous emission. The strict condition of sub-half-wavelength is relaxed extensively, which improves the experimental feasibility and controllability.

Acknowledgment

We would like to thank Prof. Hu Xiang-Ming for his valuable discussions and encouragement.

References

[1] Metcalf H and Vander Straten P 1994 *Phys. Rep.* **244** 204
[2] Chu S 1998 *Rev. Mod. Phys.* **70** 685
[3] Phillips W D 1998 *Rev. Mod. Phys.* **70** 721
[4] Liu L W, Tan L, Ding C Y, Zhang Y Q and Tan W T 2008 *Chin. Phys.* B **17** 3662
[5] Cheng H D, Wang X C, Xiao L, Zhang W Z, Liu L and Wang Y Z 2011 *Chin. Phys.* B **20** 023701
[6] Collins G P 1996 *Phys. Today* **49** 18
[7] Dalfovo F, Giorgini S, Pitaevskii L P and Stringari S 1999 *Rev. Mod. Phys.* **71** 463
[8] Mu A X, Zhou X Y and Xue J K 2008 *Chin. Phys.* B **17** 764
[9] Johnson K S, Thywissen J H, Dekker N H, Berggren K K, Chu A P, Younkin R and Prentiss M 1998 *Science* **280** 1583
[10] Scully M O and Druhl K 1982 *Phys. Rev.* A **25** 2208
[11] Storey P, Collett M and Walls D F 1992 *Phys. Rev. Lett.* **68** 472
[12] Storey P, Collett M and Walls D F 1993 *Phys. Rev.* A **47** 405
[13] Thomas J E and Wang L J 1995 *Phys. Rep.* **262** 311
[14] Rudy P, Ejnisman R and Bigelow N P 1997 *Phys. Rev. Lett.* **78** 4906
[15] Paspalakis E and Knight P L 2001 *Phys. Rev.* A **63** 065802
[16] Liu C P, Gong S Q, Cheng D C, Fan X J and Xu Z Z 2006 *Phys. Rev.* A **73** 025801
[17] Qamar S, Mehmood A and Qamar S 2009 *Phys. Rev.* A **79** 033848
[18] Xu J and Hu X M 2007 *Phys. Rev.* A **76** 013830
[19] Xu J and Hu X M 2007 *J. Phys.* B **40** 1451
[20] Xu J, Li Q, Yan W C, Chen X D and Hu X M 2008 *Phy. Lett.* A **372** 6032
[21] Herkommer A M, Schleich W P and Zubairy M S 1997 *J. Mod. Opt.* **44** 2507
[22] Qamar S, Zhu S Y and Zubairy M S 2000 *Opt. Commun.* **176** 409
[23] Ghafoor F, Qamar S and Zubairy M S 2002 *Phys. Rev.* A **65** 043819
[24] Sahrai M, Tajalli H, Kapale K T and Zubairy M S 2005 *Phys. Rev.* A **72** 013820
[25] Kapale K T and Zubairy M S 2006 *Phys. Rev.* A **73** 023813
[26] Shen W B, Xu J and Hu X M 2007 *Chin. Phys. Lett.* **24** 2583
[27] Ivanov V and Rozhdestvensky Y 2010 *Phys. Rev.* A **81** 033809
[28] Meystre P and Sargent M III 1999 *Elements of Quantum Optics* (3rd edn.) (Berlin: Springer-Verlag)
[29] Lax M 1968 *Phys. Rev.* **172** 350